Article

Using a Genetic Algorithm to Achieve Optimal Matching between PMEP and Diameter of Intake and Exhaust Throat of a High-Boost-Ratio Engine

Yindong Song [1], Yiyu Xu [1], Xiuwei Cheng [2], Ziyu Wang [2], Weiqing Zhu [2] and Xinyu Fan [1,*]

[1] School of Energy and Power Engineering, Jiangsu University of Science and Technology, Zhenjiang 212003, China; songyindong@just.edu.cn (Y.S.); 199210013@stu.just.edu.cn (Y.X.)

[2] China North Engine Research Institute, Tianjin 300400, China; xiuweicheng2008@126.com (X.C.); zealyouth2002@126.com (Z.W.); ck2828303@163.com (W.Z.)

* Correspondence: fanxy@just.edu.cn

Abstract: With the increasingly stringent CO_2 emission regulations, the degree of strengthening of the engines is increasing. Under high-pressure conditions, the airway throat parts of the intake and exhaust systems have a great influence on the flow loss of the diesel engine. The reasonable distribution of the throat area of the intake and exhaust ports in the limited cylinder headspace is key to improving the performance of supercharged engines. This study took a large-bore, high-pressure ratio diesel engine as the research object. Firstly, the three-dimensional (3D) flow simulation method was used to reveal the influence law of different throat areas on the engine intake and exhaust flow under steady-state conditions, and a steady-flow test bench was built to verify the accuracy of the simulation model and law. Secondly, based on the 3D steady-state calculation and test results, a more accurate one-dimensional simulation model was constructed, and a joint optimization simulation platform was established based on the dynamic data link library. On this basis, the mathematical description of the multi-objective optimization of airway throat size was established using machine learning methods, such as a genetic algorithm, the design domain and boundary conditions of variable parameters were clarified, and the collaborative optimization objective of integrated flow coefficient and flow loss is proposed to achieve the fast and accurate optimization of intake and exhaust throat diameters.

Keywords: CFD; high-boost-ratio engine; optimization design; genetic algorithm

1. Introduction

In recent years, due to the implementation of fuel consumption regulations, engines' degree of strengthening has increased, and their boost degree has also increased. The pressure ratio of advanced diesel engines is as high as five or more [1]. The increase in the pressure ratio can effectively increase the fresh charge into the cylinder, and improve the engine dynamics and economy, but it will also lead to a sharp increase in the flow loss during the gas exchange process, especially in the narrow space of the throat of the intake and exhaust valves, which is particularly significant [2–4]. How to quickly and reasonably distribute the throat area of the intake and exhaust ports in the highly compact cylinder headspace has become a key issue, restricting the further development of the engine [5,6]. To solve this problem, an efficient and accurate prediction model is proposed in this paper, and a fast and accurate matching of performance of a large-bore, high-pressure ratio diesel engine and intake and exhaust throat diameters is achieved.

At present, there has been some research on the influence of the intake and exhaust ports on the performance of diesel engines in the world. Liu et al. [7] studied the influence of the shape of the intake port on the flow coefficient. Li et al. [8] and Gustavo et al. [9], respectively, studied the effect of the valve seat ring diameter and intake manifold shape

on the intake air volume of the engine. Cao [10] and Wang et al. [11] optimized the air passage structure, which greatly improved the swirl ratio in the cylinder and improved the power performance of the diesel engine. Wang et al. [12] studied the effect of maximum valve lift (MVL) on the air passage, valve seat and gas flow in the cylinder through a series of experiments. Nishad et al. [13] applied large eddy simulation (LES) for evaluation and found that port and valve structures strongly influence in-cylinder turbulence characteristics. In previous studies, the influence of different intake and exhaust port throat diameters, different intake pressures, different intake pressure differences and different valve lifts on the flow coefficient of high-pressure-ratio engines is insufficient and needs further research.

In terms of optimization methods of airway structure, the design of experiment (DOE) method is usually used to establish an empirical model and the optimal scheme is obtained by optimizing the control parameters of the specific operating point of the empirical model in previous studies [14,15]. This method is time-consuming and labor-intensive, it is impossible to create models for all operating points, and it is difficult to obtain the optimal solution for the entire domain. Therefore, the combination of thermodynamic simulation calculations through intelligent optimization methods has become an effective technical approach [16–19]. Among them, the genetic algorithm (GA) has been widely used in engine operating condition optimization and external geometry optimization due to its randomness and ability to avoid becoming trapped in local minima [20,21]. Wickman et al. [22] used the KIVA code of the GA to optimize the geometry of the diesel engine combustion chamber for small and large apertures. They optimized three chamber geometry variables as well as six operating variables for both engines. Sung Wook Park et al. [23] used the GA KIVA-GA code to pre-optimize the geometry of the diesel engine stoichiometric combustion chamber, which improved the oxygen utilization and led to a 35% improvement in the fuel consumption rate. Zifei Li [24] used the simulation software BOOST to establish a one-dimensional engine model to optimize the valve phase of the engine. To reduce the development time and cost, the one-dimensional numerical simulation technology was combined with the genetic algorithm program written in MATLAB software to achieve a highly efficient multi-parameter parallel automatic optimization.

To sum up, this study combines GA and numerical simulation technology, and proposes an efficient prediction model based on a genetic algorithm, and it achieves a fast and accurate match between the performance of a large-bore high-pressure ratio diesel engine and the diameter of the intake and exhaust throats. Firstly, according to the structural parameters of the engine, several groups of 3D simulation calculation models with different throat diameters are established, the influence law of different throat areas on the engine intake and exhaust flow under steady-state conditions is studied through the simulation calculation results, the diagram of flow coefficient for different throat diameters is obtained, and the accuracy of the simulated airway model and law is verified through steady-flow bench tests. Then, based on the 3D steady-state calculation and test results, a more accurate one-dimensional thermodynamic simulation model is constructed, a simulation optimization platform is established through connection with the dynamic data link library of MATLAB/SIMULINK, and a fast and accurate optimization of intake and exhaust throat diameters is achieved by combining it with GA. Compared with the traditional optimization method, the optimization method using GA not only greatly increases the computational domain, but also reduces the computational time cost, making it more suitable for solving some complex optimization problems that cannot be handled by traditional methods, with good application prospects.

2. Analysis of Steady-State Flow Law at the Engine Port Throat

In order to study the impact of different throat sizes on the flow law of intake and exhaust passages, according to the engine structural parameters, the P/Creo 3D Computational Aided Design (CAD) software was used to establish the intake and exhaust port models with different throat structures, which were then imported into 3D CFD software for steady-state flow calculation to study the law for the influence of the throat diameter on

the flow coefficient of the intake and exhaust ports under different lifts, different intake and exhaust pressures and intake pressure differences.

2.1. Air Passage Performance Evaluation Method

The flow coefficient is an important parameter to measure the engine's intake and exhaust systems. To facilitate a comparison between the flow performance of the intake and exhaust passages with different shapes and throat sizes, the evaluation parameters defined by AVL were used, and the dimensionless flow coefficient was used to evaluate the airway circulation ability under different valve lifts.

Flow coefficient under a certain valve lift:

$$C_F = \frac{\dot{m}}{\rho_s A V_0} \tag{1}$$

Average flow coefficient during the intake process:

$$(C_{Fm})_{AVL} = \frac{1}{\sqrt{\frac{1}{\pi} \int_0^\pi \left(\frac{C_{(\alpha)}}{C_m}\right)^3 \left(\frac{1}{C_F}\right)^2 d\alpha}} \tag{2}$$

$\dot{m}$ is the measured airway flow; V_0 is the valve throat flow rate; A is the cross-sectional area of valve seat throat; $C_{(\alpha)}$ is the piston movement speed; C_m is the average piston speed.

2.2. Establishment of Engine Port Model

First, the model reference and design constraint conditions were determined according to the engine structure parameters, then the shape and size of the throat were selected and determined, and finally the design parameters of the model were determined. Different intake and exhaust port models were established according to the determined design parameters. In accordance with the principle that the total throat area of the intake and exhaust ports remains unchanged, 13 intake port models were established with a throat diameter of 39–50.5 mm, and 13 corresponding exhaust port models were established with a throat diameter of 41–52 mm. The specific throat size is shown in Table 1. The airway modification plan is shown in Figure 1a.
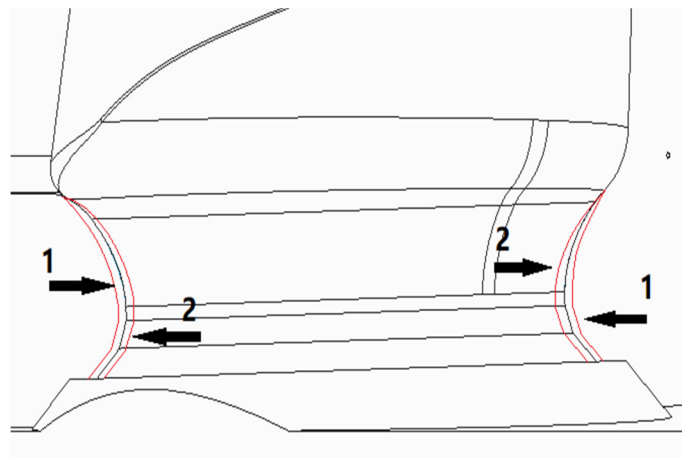
Table 1. Intake and exhaust throat size.

| Model Number	1	2	3	4	5	6	7	8	9	10	11	12	13
Intake throat diameter (mm)	39	40	41	42	43	44	45	46	47	48	49	50	50.5
Exhaust throat diameter (mm)	52	51.5	50.5	50	49	48	47	46	45	44	43	42	41

The established airway model was imported into the 3D CFD simulation software AVL-FIRE, and the mesh design was carried out through the meshing program FAME. The intake port mesh model and the exhaust port mesh model are shown in Figure 1b,c. There are many built models; mainly the fifth group of models is listed, including the intake port model with an intake throat diameter of 43 mm, and the exhaust port model with an exhaust throat diameter of 49 mm. The rest of the models were similar and will not be enumerated here.

The steady-state simulation calculation of cold fluid was carried out for inlet and exhaust ports. First, the calculation area was discretized based on the finite volume method. Taking the maximum valve lift time of the intake port of the original model as an example, different grid resolutions were selected for different calculation areas, and the calculation time and accuracy are shown in Table 2. The calculation results of schemes 1 and 2 were not suitable for convergence and were not considered. Comparing schemes 3, 4, and 5, the calculation result of scheme 3 strongly deviated from the convergence value. Considering
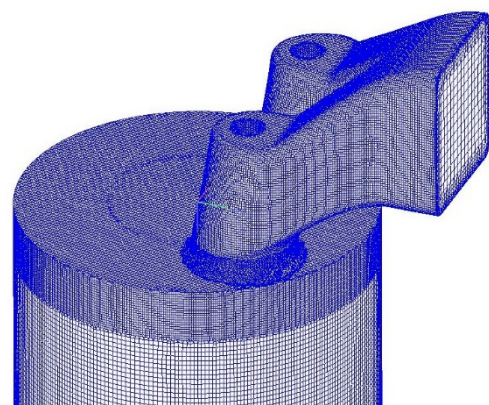
the calculation time cost and calculation accuracy, scheme 4 was the most suitable for subsequent calculation.

(**a**)
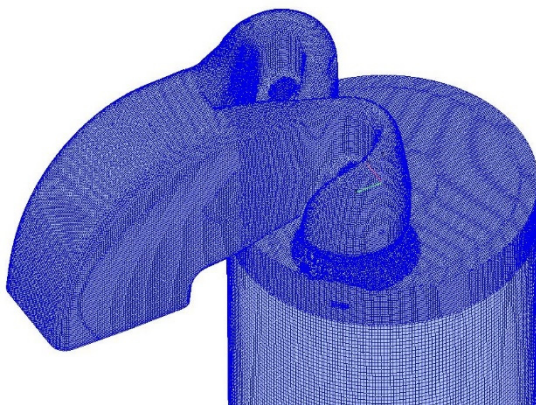
(**b**)

(**c**)

Figure 1. (**a**) Modification method of intake and exhaust throat; (**b**) intake port with a throat diameter of 43 mm; (**c**) exhaust port with a throat diameter of 49 mm.

Table 2. Meshing schemes for different areas.

Scheme	Cylinder/mm	Cylinder Head/mm	Airway/mm	Valve/mm	Valve Seat/mm	Number of Grids	Calculate Time/h
1	4	4	4	2	2	227,612	1
2	4	4	2	1	1	392,784	2
3	4	4	1	0.5	1	1,240,663	8
4	4	2	1	0.5	0.5	1,780,329	10
5	4	2	0.5	0.5	0.5	3,237,339	18

Integrate continuous equations, momentum equations and other control equations were placed in the computational grid to obtain discrete equations in the computational domain. The SIMPLE algorithm was used to discrete equations, and the algebraic equations were solved by the second-order upwind scheme. According to the law of conservation of mass, the law of conservation of momentum and the law of conservation of energy, the mass conservation equation, momentum conservation equation and energy conservation equation of 3D compressible flow were established, respectively, to form the control equation of gas flow in the airway. The turbulence model in the mainstream area adopted a

k-zeta-f four-equation turbulence model to describe the generation and consumption of turbulence, and the near-wall area was handled using standard wall functions. The range of dimensionless parameter y^+ was $30 \leq y^+ \geq 300$. The fluid temperature was set to 293.15 K. The inlet and outlet of the intake port adopted pressure boundary conditions. At the inlet section of the intake port, different total intake pressures were set, namely, 0.1 MPa, 0.2 MPa, 0.3 MPa, 0.4 MPa, 0.5 MPa, and different intake and exhaust pressure differences were set under five different total intake pressures: 2.5 kPa, 5 kPa, 10 kPa, 20 kPa, and 40 kPa, respectively. The lift nodes for simulation calculation of different throat diameter models were 1 mm, 3 mm, 5 mm, 7 mm, 9 mm, 11 mm, and 13.7 mm. The flow coefficients of each model under different working conditions were calculated, and the convergence standard of the calculation results was 0.0001.

2.3. Results and Analysis

The calculation results of about 3500 operating conditions for the above 26 models were counted, and the simulation results of the intake port of Model 4 and Model 5 were taken as examples for analysis. Figure 2a,b show the calculation results of intake throat diameters of 42 mm and 43 mm under the condition of an intake and exhaust air pressure difference of 2.5 kPa, where the *x*-axis is the intake valve lift, P_{in} is the intake pressure, and C_f is the flow coefficient.
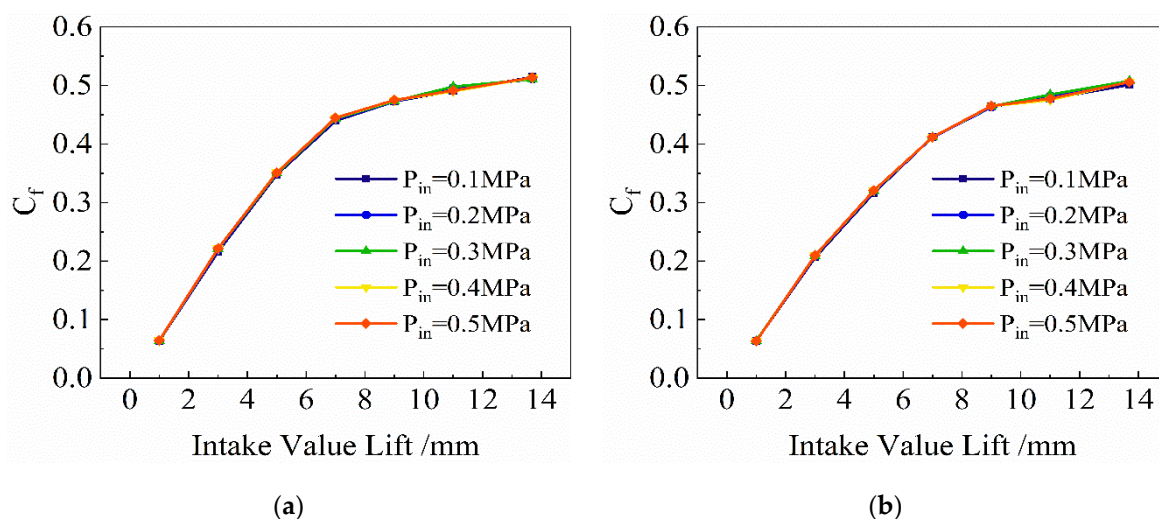

| (a) | (b) |

Figure 2. (**a**) Different intake pressure under 42 mm throat; (**b**) different intake pressure under 43 mm throat.

By analyzing the results of CFD simulation calculations in Figure 2a,b, the relationship between intake valve lift, intake pressure and flow coefficient in the intake port model under the same throat diameter and pressure difference was obtained. Under the condition of constant throat diameter, as the lift increased, the flow coefficient gradually increased, and the magnitude of the increase in flow coefficient increased from fast to slow, and gradually became gentle. Under the same intake pressure difference, the throat diameter and valve lift remained unchanged, and the flow coefficient hardly changed with the change in intake pressure in the intake port.

Figure 3a,b show the calculation results when the intake pressure was 0.1 MPa and the intake port with the same throat diameter had different pressure differences and lifts. ΔP is the intake and exhaust pressure difference.

Through an analysis of the CFD simulation calculation results of Figure 3a,b, it can be seen that, under a constant throat diameter and intake pressure, the flow coefficient under the same lift hardly changed with the change in the intake and exhaust pressure difference. Except for the models with 42 mm and 43 mm intake throat diameters, the simulation cal-

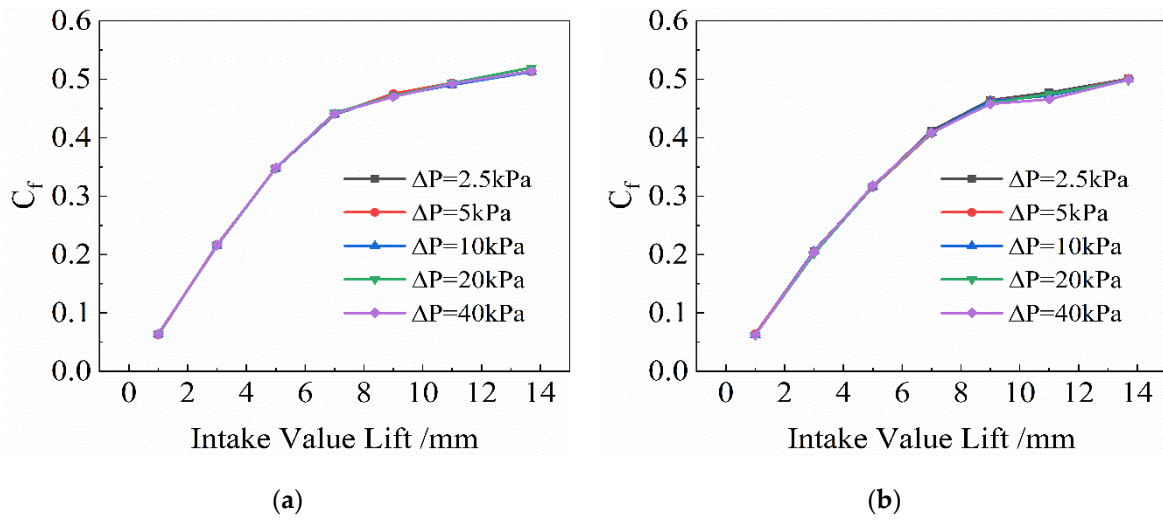culation results of intake and exhaust port models under other throat diameters displayed the same law.

(**a**)

(**b**)

Figure 3. (**a**) Different intake pressure differences under 42 mm throat; (**b**) different intake pressure differences under 43 mm throat.

According to these laws, the maps of throat diameter, valve lift and flow coefficient are listed, showing different intake and exhaust pressure and differential pressure conditions. D_{in} and D_{out} are the inlet throat diameter and the exhaust throat diameter, as shown in Figure 4a,b.

Through the analysis of the intake and exhaust port flow coefficients in Figure 4a,b, it can be seen that, regardless of intake or exhaust port, under the same throat diameter, the flow coefficient is proportional to the valve lift, and as the valve lift decreases, the flow coefficient decreases more quickly. In addition, under the same valve lift, with the increase in the diameter of the intake and exhaust throats, the flow coefficients present a gradual decreasing trend. In this paper, the flow coefficient defined by AVL was used as the airway performance evaluation parameter. According to the calculation, the decrease in the flow coefficient is because when the throat diameter increases, the theoretical mass flow rate increases faster than the actual calculated mass flow rate. Hence, there is a law that the average flow coefficient decreases as the throat diameter increases.
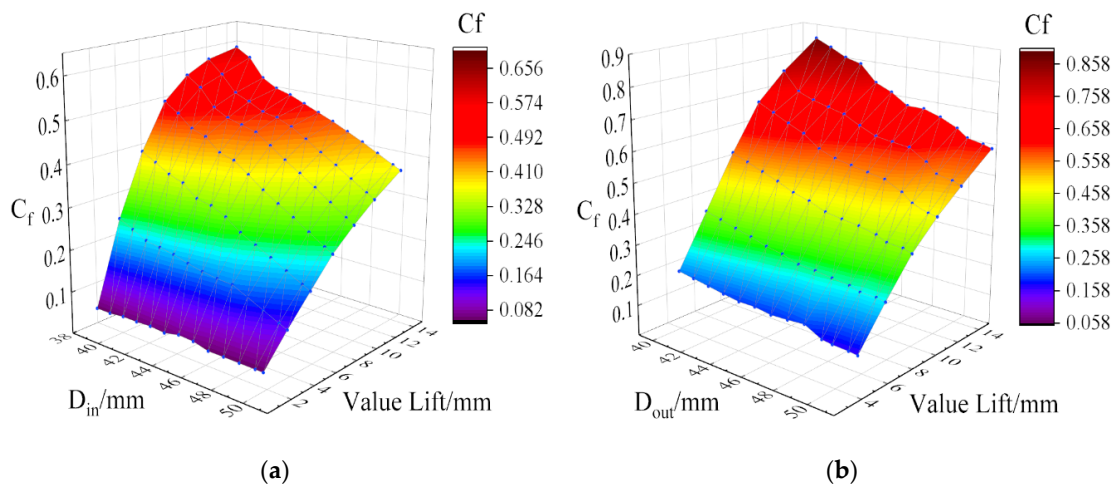

(**a**)

(**b**)

Figure 4. (**a**) Map diagram of intake throat diameter, valve lift, and flow coefficient; (**b**) map diagram of exhaust throat diameter, valve lift, and flow coefficient.

3. Test System and Method

3.1. Test Equipment

To verify the accuracy of the CFD simulation model, the AVL TIPPELMANN test bench was used to carry out a steady-flow airflow test. The test bench included the test bench table, the stabilized voltage cylinder, the intake and exhaust pipes, conversion control valve, centrifugal fan, impeller anemometer, data acquisition instrument, computer, etc., as shown in Figure 5a. Figure 5b is the physical image of the engine port steady-flow test bench.
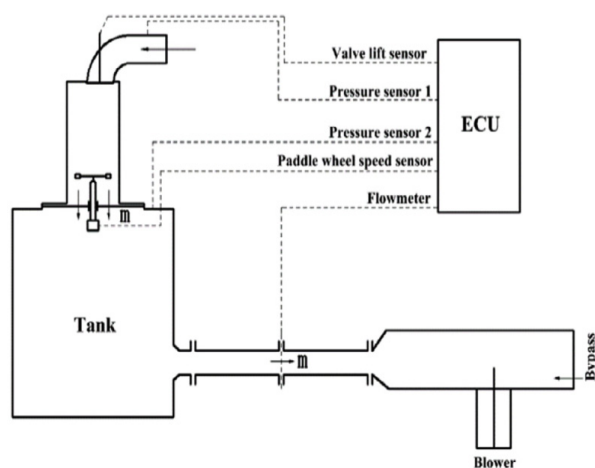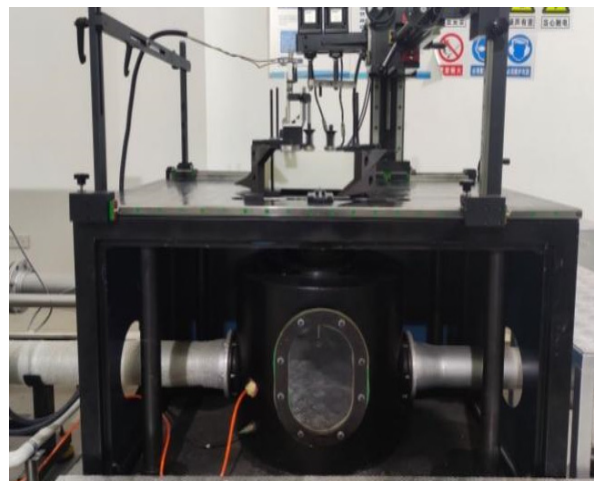
(**a**) (**b**)

Figure 5. (**a**) Principle diagram of the engine port steady flow test bench; (**b**) physical image of the engine port steady flow test bench.

Intake and exhaust port simulation models of some caliber were selected to make test core boxes for testing. The test core boxes were manufactured using 3D printing technology. There were 6 in total, including 12 different intake and exhaust throat diameters, as shown in Table 3. The actual airway core box is shown in Figure 6.

The steady-flow test was carried out for the cylinder head intake and exhaust ports in accordance with the method in which the pressure difference was set as 5 kPa according to blade mode and differential pressure measurement, and the gas flow direction was consistent with the actual intake and exhaust flow direction of the engine. The flow conditions in the intake and exhaust ports were measured under different valve lifts, and the dimensionless flow coefficient was calculated based on the measured parameters. The basic parameters and accuracy requirements for the measuring instruments used in the experiment are shown in Table 4.

In the steady air-flow test, the starting lift point of the intake and exhaust port was 0, the lift measurement points of the intake port were 1 mm, 3 mm, 5 mm, 7 mm, 9 mm, 11 mm, and 13.7 mm, and the lift measurement points of the exhaust port were 3 mm. 5 mm, 7 mm, 9 mm, 11 mm, and 13.7 mm. The computer controlled the valve lift of the intake and exhaust ports through the lift sensor and collected the corresponding experimental data under each lift. To guarantee the accuracy of the experimental data, the intake and exhaust ports of each core box were subjected to three repeatability tests. The cylinder head was removed and reinstalled in each test, and it was guaranteed that the error of the three measurements was less than 3%.

Table 3. Throat size of intake and exhaust core box.

Model Number	3	4	5	6	7	8
Intake throat diameter (mm)	41	42	43	44	45	46
Exhaust throat diameter (mm)	50.5	50	49	48	47	46
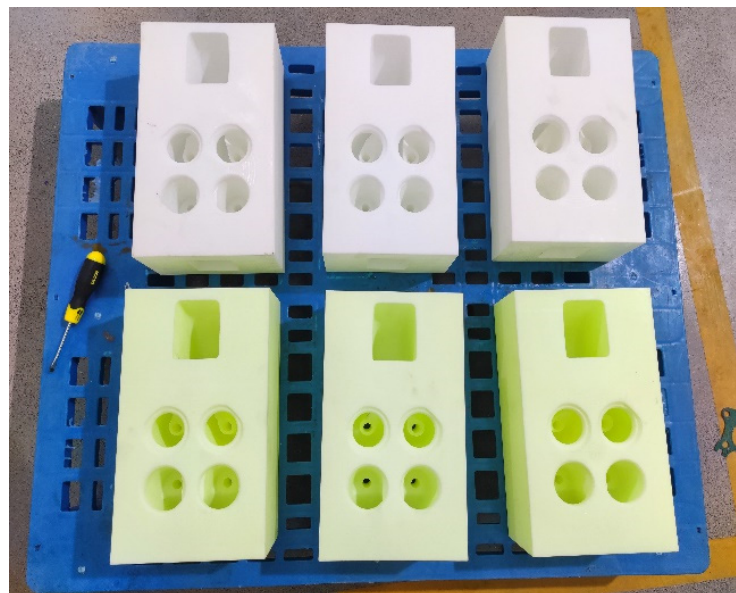
Figure 6. The physical diagram of the intake and exhaust core box with different throat diameters.

Table 4. Accuracy requirements of test equipment.

Serial Number	Test Instrument	Parameter	Range Ability	Instrument Accuracy
1	Flow meter	Flow rate	(5~5200) kg/h	±1.0%
2	Pressure sensor	Differential pressure	(1~15) kPa	±0.3%
3	Temperature sensor	Temperature	(0~100) °C	±0.25 °C
4	Airflow speed sensor	Rotation speed	(0~30,000) r/min	≤4%

3.2. Statistics and Error Comparison of Test Results

To reduce the impact of the test bench or the operator on the test data during the test, at least three tests were carried out on the intake and exhaust ports of each cylinder head, and the test data that met the error conditions were averaged as the basic data of the test. The sorted experimental data of the intake and exhaust ports regarding the throat and lift are shown in Figure 7a,b.

It can be seen from Figure 7a,b that, under the same lift conditions, with an increase in throat diameters in the intake and exhaust port models, the flow coefficient tends to gradually decrease, which is consistent with the law of CFD simulation calculation. To more intuitively see the relationship between the test value and the simulation value, Figure 8a–d list the test and simulation data of models 7 and 8.

The comparison data graph shown above demonstrates that both the flow coefficient measured by the steady-state experiment and the flow coefficient calculated by the CFD simulation display the same law. The throat diameter is constant, and the flow coefficient increases with the increasing lift. The increasing speed is first fast and then slow, with a gradual tendency to flatten. In addition, the test results are in good agreement with simulation calculation results under various working conditions. Comparing all model tests and simulation errors, the error of the intake port is within 10%, and the error of the exhaust port is basically within 5%. This not only verifies the correctness of the simulation

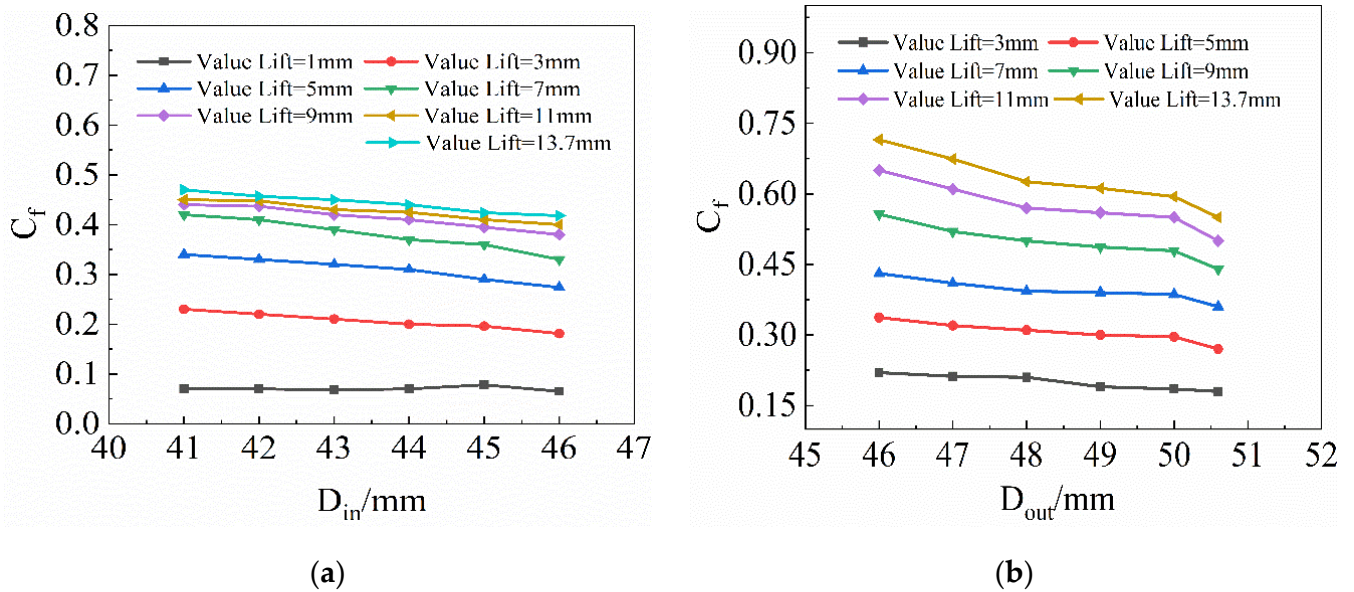calculation model but also provides reliable support for the subsequent one-dimensional modeling and analysis.

(**a**)	(**b**)

Figure 7. (**a**) Test results of different throat intake ports; (**b**) test results of different throat exhaust port.

It can also be seen from the results that, when the throat diameter is constant, the larger the valve lift, the larger the error of the intake port, while the overall distribution of the error of the exhaust port is relatively uniform. The main reason for this phenomenon is that the intake port is spiral, and the intake process is complicated. Therefore, when the large lift intake volume is high, there is a high level of actual loss of the intake port. In addition, when performing CFD simulation calculations on the 3D model, if a mathematical model is used to simulate the actual flow state, it cannot accurately reflect the gas flow state during the actual intake process, and certain errors will occur. Errors caused by the human operation process of the experimenter or by the measurement accuracy of the measuring instrument are inevitable.
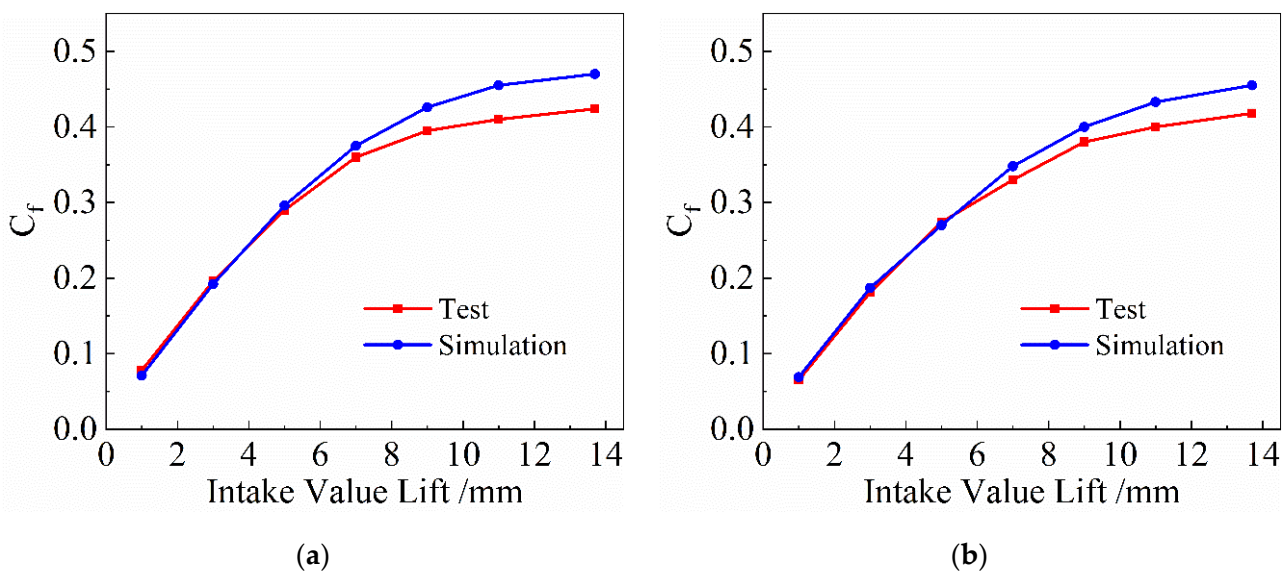

(**a**)	(**b**)
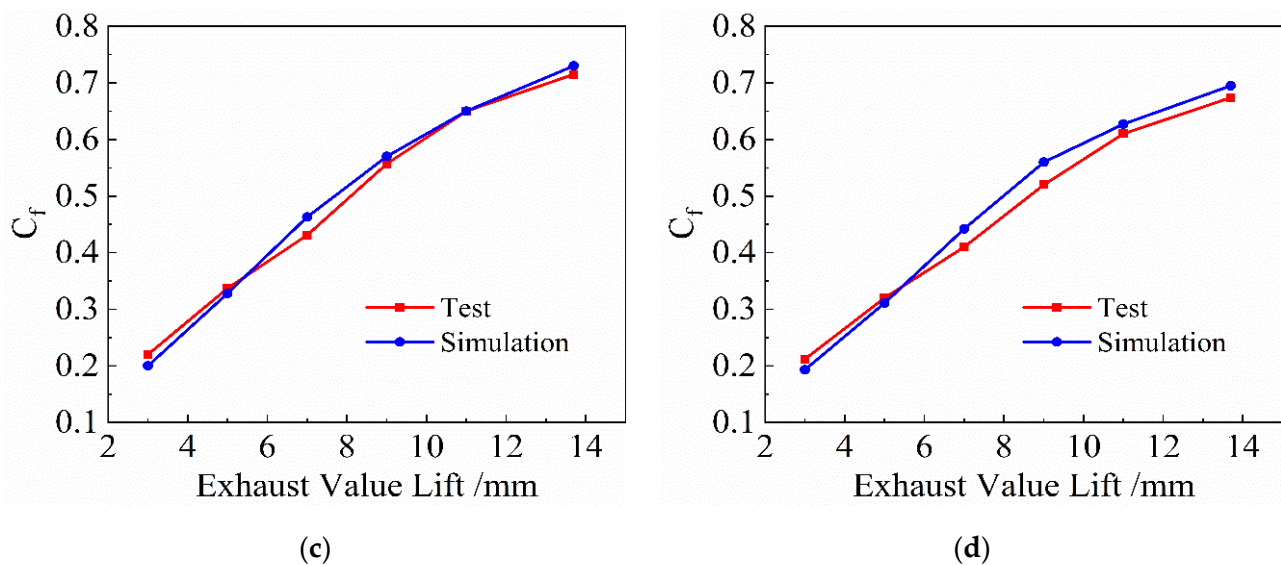
Figure 8. *Cont.*

(**c**)

(**d**)

Figure 8. (**a**) Comparison of test and simulation results of 45 mm-throat intake port; (**b**) comparison of test and simulation results of 46 mm-throat intake port; (**c**) comparison of test and simulation results of 46 mm-throat exhaust port; (**d**) comparison of test and simulation results of 47 mm-throat exhaust port.

4. Optimization of Throat Diameter

The optimization of the engine intake and exhaust throat is a multi-parameter, multi-objective, nonlinear problem. To reduce development costs, a joint simulation optimization method is proposed, which combines the basic parameters of the engine model to establish a GT-Power simulation calculation model for the engine working process. GT-Power provides a dynamic data link library interface with MATLAB/SIMULINK. For the problems that need to be optimized, the GA program is compiled using MATLAB software, and the operating parameters of the engine in the GT-Power simulation model are controlled and calculated through the SIMULINK module to establish the SIMULINK/GT-Power engine joint simulation optimization platform, so that the diameter of the intake, the exhaust throat, is quickly and accurately optimized.

4.1. Establishment and Verification of One-Dimensional Simulation Model

As a one-dimensional simulation software developed by Gamma Technologies, GT-Power is currently widely used in CFD simulation of automobile engines. Key computer-aided engineering (CAE) parameters are collected through engine port and cylinder block models and reasonably simplified. The pipeline system is divided into several control volumes to establish a single-cylinder, one-dimensional simulation model based on the engine port and cylinder flow and combustion laws. CAE key parameters are shown in Table 5.

Table 5. Key parameters of engine computer aided engineering (CAE).

Parameter	Value	Parameter	Value
Number of cylinders	1	Number of valves	4
Cylinder diameter (mm)	150	Intake valve diameter (mm)	44
Connecting rod length (mm)	290	Exhaust valve diameter (mm)	48
Number of injectors	10	Injector diameter (mm)	0.35
Clearance height (mm)	1.5	Injection cone angle (°)	153
Stroke (mm)	150	Inlet valve clearance (mm)	0.5
Compression ratio	14.735	Exhaust valve clearance (mm)	0.5

The single-cylinder simulation model, established according to Table 5, is shown in Figure 9:
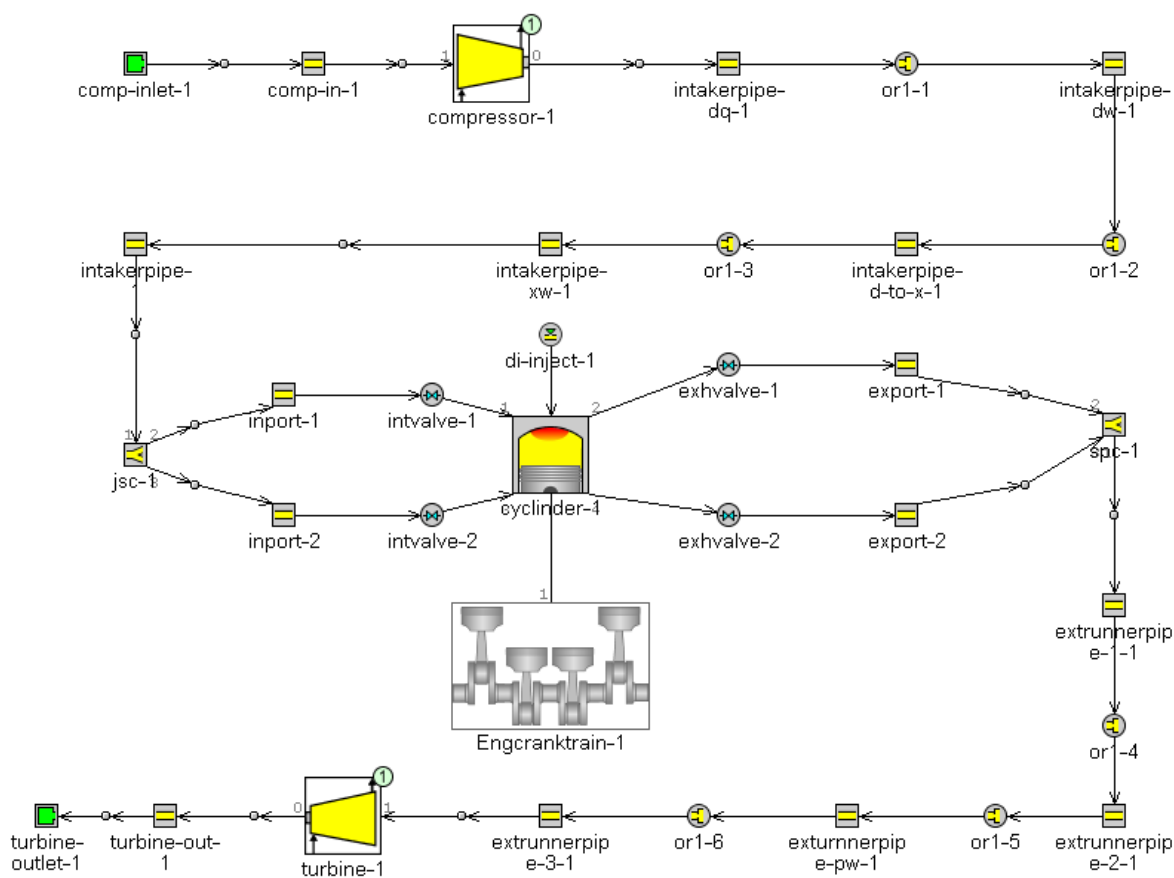

Figure 9. GT-Power one-dimensional simulation model.

The correctness of the established one-dimensional model directly affects the subsequent calculation results. Therefore, the established model needs to be checked and calculated based on the existing engine experimental data. Parameters such as the checkpoint rotation speed, intake, and exhaust pressures of the simulation model are all experimental values. The main performance parameters of the experimental value and the simulation value, and the size of the error are shown in Table 6. Pe is the effective power, Be is the effective specific fuel consumption, and the IMEP is indicated mean effective pressure.

Table 6. Comparison of simulation and test performance indicators of checkpoints.

Parameter	Torque (N*m)	Pe (kW)	Be (g/kW*h)	IMEP (MPa)
Simulation value	498.9	114.9	241.1	2.90
Test value	490.4	110.7	246.3	2.87
Error	1.7%	3.8%	2.1%	1.0%

From the comparison of the performance parameters in simulation results and test results in Table 6, it can be seen that there is a certain error between the test value and the simulation value. For this reason, the simulation model uses the mathematical model to replace the real combustion, which is not exactly the same as the actual combustion in the cylinder. It can also be seen from the above table that the error size of each performance parameter is within 5%, which fully meets the requirements of establishing a simulation model, so it is confirmed that the GT-Power one-dimensional simulation model is established correctly and can be used for subsequent simulation calculations.

4.2. Optimization Method Based on Genetic Algorithm (GA)

Corresponding with the 3D simulation model established above, 13 sets of GT-Power simulation models were established, with different intake and exhaust throat diameters. Based on the flow coefficients corresponding the to different intake and exhaust throat diameters calculated in the above 3D simulation, 78 sets of GT-Power single-cylinder simulation models were established, with a pressure ratio of 1:6. To better analyze and describe the influence of different intake and exhaust throat ratios, the pumping mean effective pressure (PMEP) was selected as a characteristic parameter to quantitatively characterize the engine performance.

The GT-Power single-cylinder simulation model was combined with the SIMULINK module in MATLAB software, and the input parameters were controlled in the GT-Power single-cylinder simulation model by using MATLAB to compile GA programs, thus establishing the SIMULINK/GT-Power engine joint simulation optimization platform. The programmed GA program flow is shown in Figure 10.

Genetic algorithm mechanism: First, the problem to be solved was encoded and expressed it in the form of binary strings, also called chromosomes. The chromosomes of a certain scale form a population, and the initial population was randomly generated by the computer in a predetermined search space. According to the survival of the fittest principle, individuals with better objective function values in the population were selected. These excellent individuals generated the next generation through genetic manipulation to constitute a new population. After a certain number of evolutions, the final population converged to the optimal function value. To make the variables converge before the number of iterations is reached, the discrete and random initial population was set with a scale of 20, chromosome length of 7, generation gap of 0.8, and genetic algebra of 15. When the number of iterations in the GA reached the set maximum evolutionary algebra, or when the optimal solution obtained did not change despite several generations of continuous evolution, the iteration process was terminated.

Figure 11 shows the established SIMULINK/GT-Power engine joint simulation optimization platform, which consists of four parts. The intelligent optimization module is the main body of the joint simulation optimization platform, which is mainly composed of GA programs. The program can iteratively optimize different combinations of intake and exhaust throats under different working conditions and determine the choice of intake and exhaust throat diameters according to the returned target value. The 3D simulation data module calculates and outputs the flow coefficient of the new model based on the previous engine 3D CFD simulation results. The role of the parameter transmission interface module is to provide channels to transmit data, such as intake and exhaust throat parameters and flow coefficients, to the SUITE engine cycle calculation module. The primary role of the engine cycle calculation module is to invoke the GT-SUITE main program and calculate and return the engine performance evaluation parameters under different conditions.
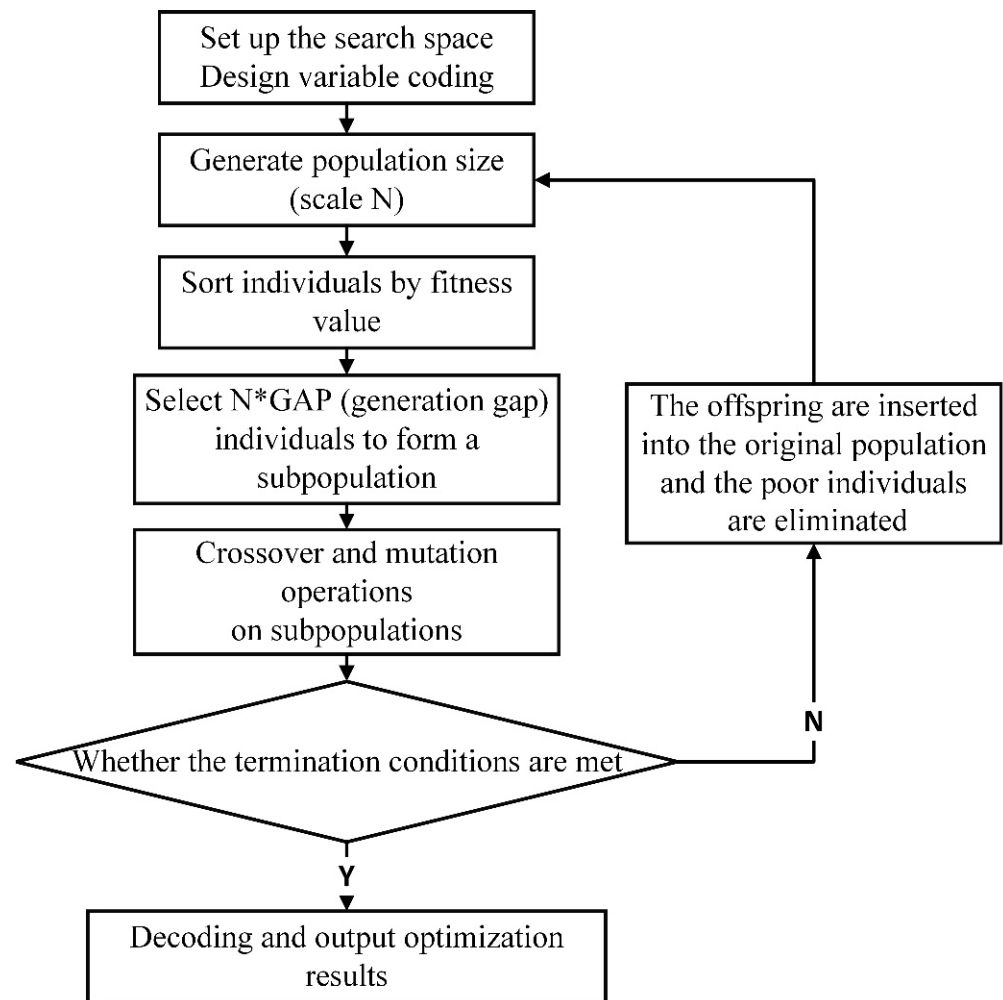
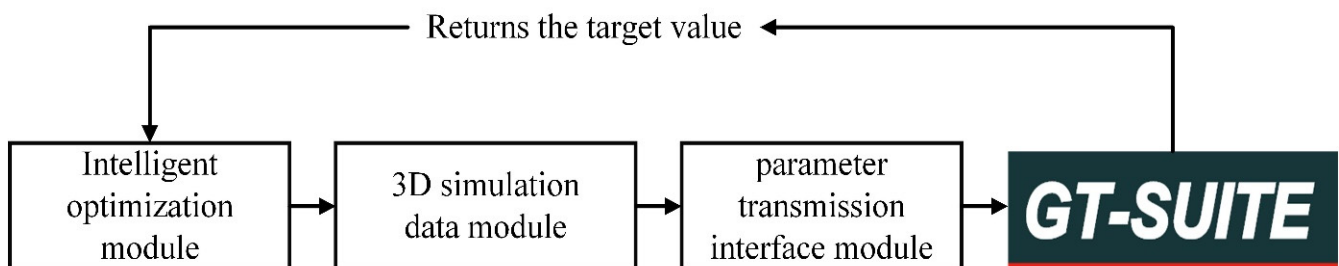**Figure 10.** Operational steps in genetic algorithm design.

Figure 11. Implementation method of the joint simulation optimization platform.

After the joint simulation optimization platform was established, the measurement points were selected according to the GT-Power simulation model that was modeled and calculated above, and the PMEP was used as the evaluation parameter to check the correctness of the optimization platform. The errors of the values calculated by the GT-Power simulation model and the joint simulation optimization platform were all within 0.5%, which meets the requirements of subsequent calculations.

4.3. Result Analysis

Figure 12a–f show the calculation results of 78 GT-Power single-cylinder models with pressure ratio of 1:6.
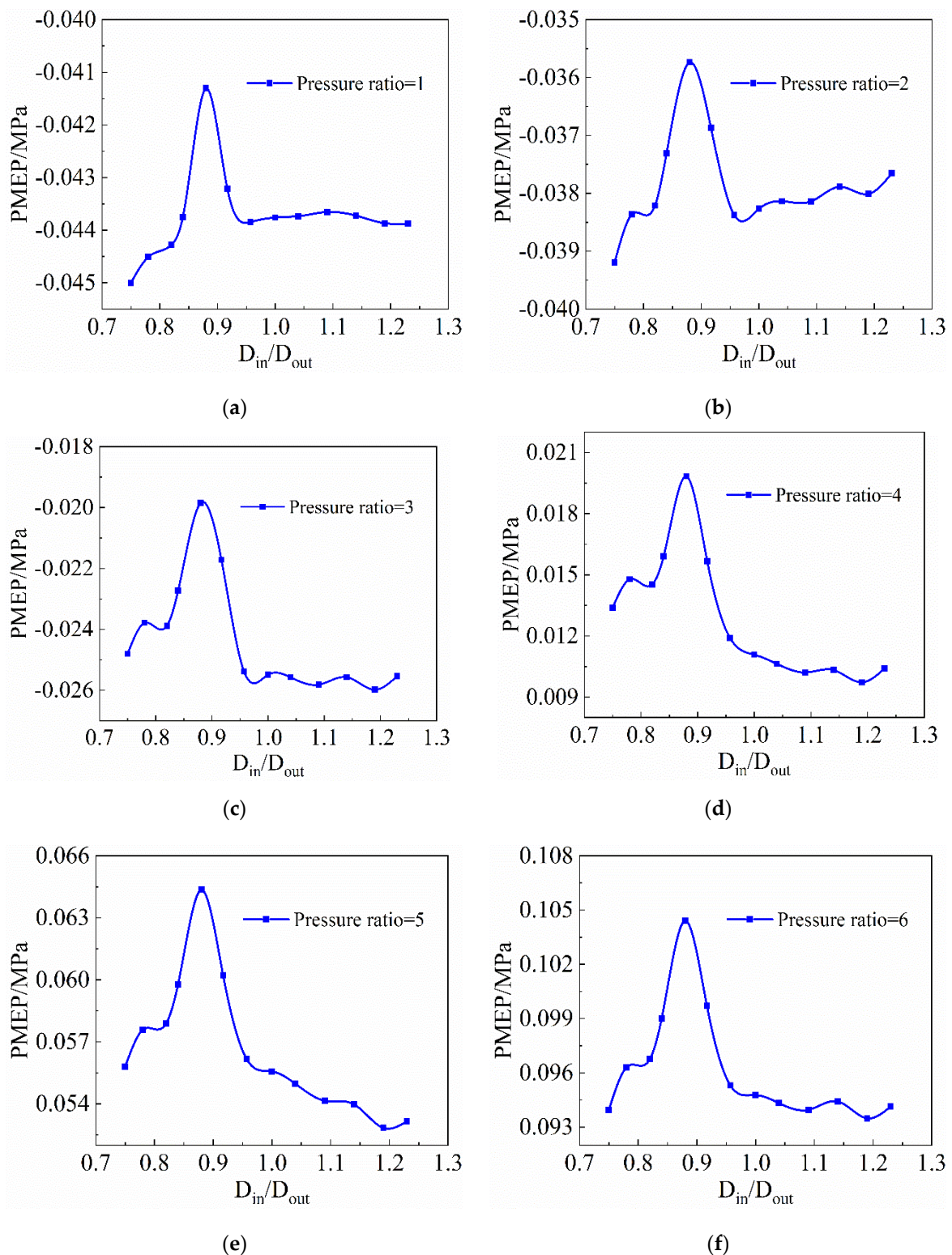
Figure 12. (**a**) PMEP under pressure ratio 1; (**b**) PMEP under pressure ratio 2; (**c**) PMEP under pressure ratio 3; (**d**) PMEP under pressure ratio 4; (**e**) PMEP under pressure ratio 5; (**f**) PMEP under pressure ratio 6.

From the above calculation results, it can be seen that when the pressure ratio is 1, 2, or 3, the PMEP is less than zero and negative work is carried out. The smaller the absolute value of PMEP, the better the engine performance. When the pressure ratio is 4, 5, or 6, the PMEP is greater than zero and positive work is carried out. The greater the absolute

value of the PMEP, the better the engine performance. By analyzing the above manual optimization calculation results of different pressure ratios, it is finally determined that the ratio of the optimal intake throat diameter to the exhaust throat diameter is 0.88. That is, the intake throat diameter is 43 mm, and the exhaust throat diameter is 49 mm.

After the establishment of the SIMULINK/GT-Power engine joint simulation optimization platform, the distribution of the inlet throat diameter, and the PMEP of the initial population and the last population when the pressure ratio calculated by the GA program is 1, are shown in Figure 13.
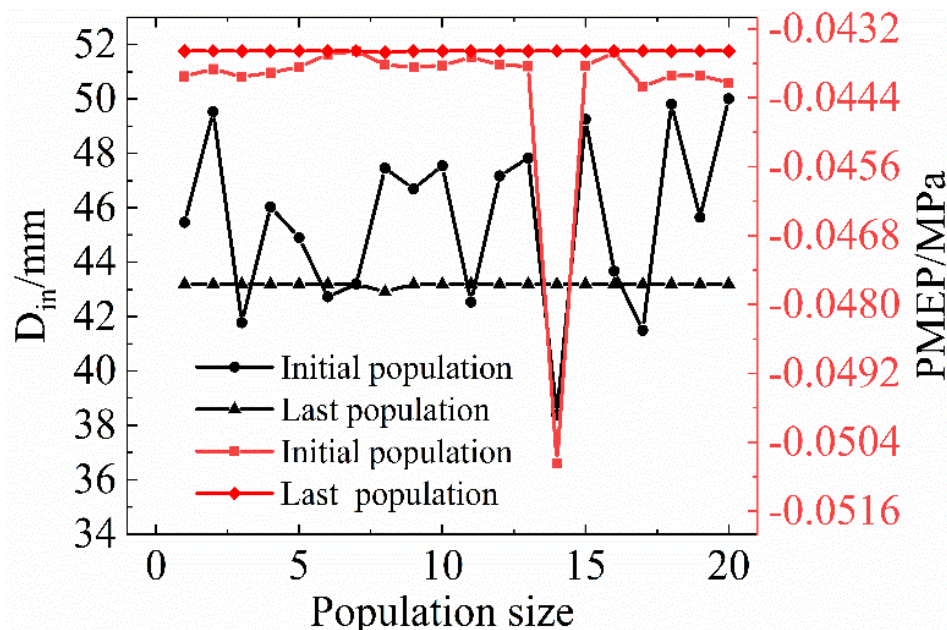

Figure 13. Distribution map of the initial population and the last population.

It can be seen from the figure that the initial combination of intake and exhaust throat diameters is randomly generated within a given range by the GA program. The initial population was scattered in the entire search space. After a certain number of genetic and iterative calculations, the variable result tends to be stable, and the combination of intake and exhaust throat diameters converges to a fixed value. The GA method was used to calculate the different pressure ratios. The results of the joint simulation optimization method and the manual optimization method under each pressure ratio condition are shown in Table 7.

Table 7. Comparison of joint simulation optimization results and manual optimization results.

Pressure Ratio	Optimization Method	1	2	3	4	5	6
Intake throat diameter (mm)	Joint simulation	43.198	43.008	42.819	42.819	43.291	42.819
	Manual	43	43	43	43	43	43
	Error	0.46%	0.02%	−0.42%	−0.42%	0.68%	−0.42%
Exhaust throat diameter (mm)	Joint simulation	48.724	48.891	49.057	49.057	48.640	49.057
	Manual	49	49	49	49	49	49
	Error	−0.56%	−0.22%	0.12%	0.12%	−0.73%	0.12%

It can be seen from the above table that the calculation optimization results of the joint simulation platform using GA are very close to the optimization results of manual optimization, and the difference between the two optimization results is less than 0.7%, which further verifies the correctness of the joint simulation calculation platform. Compared with manual optimization, joint simulation not only provides more accurate optimization

results but also supports an autonomous and quick finding of the best matching scheme, which greatly saves time costs and speeds up the engine development process. The method of joint simulation optimization can be further extended to the optimization of other engine parameters.

5. Conclusions

For high-boost-ratio diesel engines, this paper focuses on the key issues, such as the influence law of intake and exhaust ports with different throat diameters on flow coefficient and the interaction relationship between the airway throat area ratio and the flow loss and establishes an efficient and accurate simulation platform and method for the joint optimization of airway throat size by integrating machine learning theory. The research results are as follows:

(1) A 3D steady-state simulation model is established for a diesel engine with different throat diameters, and the MAP diagrams of flow coefficient are calculated for different pressure ratios, different pressure differences and different valve lifts. On this basis, an accurate one-dimensional simulation calculation model is constructed, and 13 groups of models with different intake and exhaust throat diameters are manually calculated and optimized. The calculation results show that when the intake throat diameter is 43 mm and the exhaust throat diameter is 49 mm, the engine flow loss is the smallest and the performance is the best.

(2) According to the dynamic data link library method, a joint optimization simulation platform is established by integrating the one-dimensional simulation model and MAT-LAB/SIMULINK, and the mathematical description of the multi-objective optimization of the airway throat size is established by embedding the genetic algorithm, the design domain and boundary conditions of the variable parameters at the throat are clarified, and the flow coefficient and flow loss are integrated to optimize the solution to the target. The calculation results are more accurate compared with the manual optimization results, and the optimization period is also greatly reduced without loss of generality, meaning that it can be extended to the field of efficient optimization design of internal combustion engines.

In addition to the above research, a 3D dynamic combustion simulation model will be established next, a physical prototype will be manufactured to conduct a series of combustion experiments, and the in-cylinder combustion and flow field changes of engine models with different throat diameters will be compared and studied to further verify the correctness of the joint simulation optimization platform.

6. Prospects

(1) The mapping mechanism for the size of the intake and exhaust throats, valve lift, and flow characteristics of the high-pressure-ratio diesel engine formed in this project is not only suitable for this type of prototype but also for other diesel engines and has a certain generality.

(2) The engine co-simulation optimization platform and method established in this project, combined with the data-driven theory, can realize the accurate and efficient optimization design of throat size with multi-objective and multi-parameters, which is of great significance for guiding the optimal design of diesel engines.

Author Contributions: Conceptualization, Y.S., Y.X. and X.F.; funding acquisition, Y.S. and X.F.; investigation, Y.X. and W.Z.; methodology, Y.S. and Y.X.; project administration, Y.S., Y.X. and X.F.; resources, X.C. and Z.W.; software, Y.X. and X.F.; validation, Y.X. and W.Z.; writing—original draft, Y.X.; writing—review and editing, Y.S., Z.W. and X.F. All authors have read and agreed to the published version of the manuscript.

Institutional Review Board Statement: Not applicable.

Informed Consent Statement: Not applicable.

Data Availability Statement: The data presented in this study are available on request from the corresponding author. The data are not publicly available due to some models involved confidentiality.

Conflicts of Interest: The authors declare no conflict of interest. The funders had no role in the design of the study; in the collection, analyses, or interpretation of data; in the writing of the manuscript, or in the decision to publish the results.

References

1. Wang, T.Y. Study on the flow characteristics of the inlet ports and incylinder for internal combustion engine. *J. Eng. Thermophys.* **2008**, *29*, 693–697.
2. Zhu, R. Study of Optimized Matching of Two-Stage Turbocharging and EGR System of Heavy-Duty Diesel Engine. Master's Thesis, Jilin University, Changchun, China, 2015.
3. Li, B. Research on performance matching of intake and exhaust ports of marine medium speed dual fuel engine. *Energy Rep.* **2021**, *7*, 72–83. [CrossRef]
4. Fan, X.; Chang, S.; Lu, J. Energy consumption investigation of electromagnetic valve train at gas pressure conditions. *Appl. Therm. Eng.* **2019**, *146*, 768–774. [CrossRef]
5. Wu, H. Research and Optimize on Structure Parameters of Helical Intake Port for Diesel Engine. Master's Thesis, Huazhong University of Science & Technology, Wuhan, China, 2006.
6. Jia, M.Q. Numerical Investigation of Flow Characteristics around Intake Valve in a Supercharged Diesel Engine. Master's Thesis, Tianjin University, Tianjin, China, 2018.
7. Liu, S.J.; Zeng, J.J.; Han, W.; Chen, Y.; Wang, J. Intake and Exhaust System Performance of Diesel Engine Based on CFD and Steady Flow Test Method. *Trans. CSICE* **2016**, *34*, 68–73.
8. Li, X.Y. Study of Turbo-Charged Diesel Engine Intake and Exhaust Process Sensitivity Based on Surrogate Model. Master's Thesis, Beijing Institute of Technology, Beijing, China, 2016.
9. Gustavo, R.S.; Cláudio, C.P.; Sérgio, L.F.; Felipe, S.P. Study of intake manifolds of an internal combustion engine: A new geometry based on experimental results and numerical simulations. *Therm. Sci. Eng. Prog.* **2019**, *9*, 248–258.
10. Cao, R.X. Simulation Study on Air Flow and Combustion Process in Highly Intensified Diesel Engine. Master's Thesis, North University of China, Taiyuan, China, 2020.
11. Wang, G.; Yu, W.; Li, X.; Yang, R. Influence of fuel injection and intake port on combustion characteristics of controllable intake swirl diesel engine. *Fuel* **2012**, *262*, 116548. [CrossRef]
12. Wang, T.; Liu, D.; Wang, G.; Tan, B.; Peng, Z. Effects of Variable Valve Lift on In-Cylinder Air Motion. *Energies* **2015**, *8*, 13778–13795. [CrossRef]
13. Nishad, K.; Ries, F.; Li, Y.; Sadiki, A. Numerical Investigation of Flow through a Valve during Charge Intake in a DISI-Engine Using Large Eddy Simulation. *Energies* **2019**, *12*, 2620. [CrossRef]
14. Castagné, M.; Bentolila, Y.; Chaudoye, F.; Hallé, A.; Nicolas, F.; Sinoquet, D. Comparison of Engine Calibration Methods Based on Design of Experiments (DoE). *Oil Gas Sci. Technol.* **2008**, *63*, 563–582. [CrossRef]
15. Millo, F.; Arya, P.; Mallamo, F. Optimization of Automotive Diesel Engine Calibration Using Genetic Algorithm Techniques. *Energy* **2018**, *158*, 807–819. [CrossRef]
16. Cirak, B.; Demirtas, S. An application of artificial neural network for predicting engine torque in a biodiesel engine. *Am. J. Energy Res.* **2014**, *2*, 74–80. [CrossRef]
17. Castresana, J.; Gabia, G.; Martin, L.; Uriondo, Z. Comparative performance and emissions assessments of a single-cylinder diesel engine using artificial neural network and thermodynamic simulation. *Appl. Therm. Eng.* **2020**, *185*, 116343. [CrossRef]
18. Liu, J.; Ma, B.; Zhao, H. Combustion parameters optimization of a diesel/natural gas dual fuel engine using genetic algorithm. *Fuel* **2020**, *260*, 116365. [CrossRef]
19. Ma, X.; Song, Y.; Wang, Y.; Zhang, Y.; Xu, J.; Yao, S. Experimental study of boiling heat transfer for a novel type of GNP-Fe_3O_4 hybrid nanofluids blended with different nanoparticles. *Powder Technol.* **2021**, *396*, 92–112. [CrossRef]
20. Jing, Z.; Zhang, C.; Cai, P.; Li, Y.; Chen, Z.; Li, S.; Lu, A. Multiple-objective optimization of a methanol/diesel reactivity controlled compression ignition engine based on non-dominated sorting genetic algorithm-II. *Fuel* **2021**, *300*, 120953. [CrossRef]
21. Park, S.W.; Reitz, R.D. Numerical study on the low emission window of homogeneous charge compression ignition diesel combustion. *Combust. Sci. Technol.* **2007**, *179*, 2279–2307. [CrossRef]
22. Wickman, D.D.; Senecal, P.K.; Reitz, R.D. Diesel engine combustion chamber geometry optimization using genetic algorithms and multi-dimensional spray and combustion modeling. *SAE Tech. Pap.* **2001**, *110*, 487–507.
23. Park, S.W. Optimization of combustion chamber geometry for stoichiometric diesel combustion using a micro genetic algorithm. *Fuel Process. Technol.* **2010**, *91*, 1742–1752. [CrossRef]
24. Li, Z. Optimization of Engine Valve Phase Based on Electromagnetic Drive Valve. Master's Thesis, Nanjing University of Science and Technology, Nanjing, China, 2011.